IJESRT
INTERNATIONAL JOURNAL OF ENGINEERING SCIENCES & RESEARCH TECHNOLOGY

# Influence of Pressure Angle in Spur Gear Vibration

**Rameshbabu Subramanian[*1], Srinivasan K[2]**
[*1]Arulmigu Meenakshi Amman College of Engineering, Tamilnadu, India
[2]Anna University, India
jairameshbabu@gmail.com

## Abstract

Spur Gear vibration is one of the major indispensable parameter in Maintenance division of an operating plant. Many methods have been adopted to control the vibration in gears. An approach of understanding the influence of pressure angle in spur gear vibration is required in the modern trends. Pressure angle influence in root stress has been analyzed earlier by some of the researchers, but may not be in vibration. Three steel spur gears having the pressure angle of 14½0, 200 and 250 with the same face width, pitch circle diameter and number of teeth are selected for this analysis. The gears are loaded with a torque of 6.25, 12.5, 18.75, 25, 38 and 50Nm respectively. Loads are given as a transmitted and radial force on the gear tooth. A frequency response analysis has been done on the above gear using FEA Software. The result shows that gear having 200 pressure angle is more effective in controlling the vibration than the other two pressure angles. Also gear having 250 is also being effective in controlling the vibration than the gear having 14½0. From this interpretation, it is concluded that even a small manufacturing error which leads to pressure angle variation influences more in gear vibration.

**Keywords**: Spur Gear, Pressure Angle Influence, Vibration Analysis, Frequency Response, Finite Element Method.

## 1 Introduction

Rotating Elements in Machineries leads to more vibrations. Even very small error in system could leads to poor quality performance. Among those rotating elements, gears are prone to more vibration since the meshing frequency of the gear is the product of number of teeth with that of the speed. In gears, spur gears are being used for transmitting more power as well as with very high speed. Many research works has been carried out in analyzing the root stress, contact stress, vibration and condition monitoring of a spur gear. The spur gear vibration can be controlled by active or passive way. These types of gears will have more transverse and torsional vibration due to transmitted and radial force. Vibration which occurs in gears can be experimentally measured by using an FFT / Spectrum analyzer. The level of vibration in gears is usually measured in the near bearings of the gear shaft. The frequency report shows the magnitude of vibration of gear at its meshing frequency and its multiples. Also if it is more than two or three type of gears are tested, then the peaks can also be considered for the measurement of vibration level of the gears, provided the measurement set up remains same for the all the gears. Profile modifications, tooth asymmetry and error in profile [2, 3, 4, 5, 6 and10] has been analyzed by many researches which has certain influence in vibration control. Contact analysis and Non-linear dynamics [7, 8, 9 and 11] of gears and its influences have also been analyzed by some of the authors. Bearing deformation has been considered in some analysis [01]. Various gear parameters and its influence has also been analyzed for vibration. Vibration can be controlled by source or path or at sink or in all the three modes. Here in this work, an approach has been done to rectify at source by means of rectification in pressure angle. These types of approaches are similar to that of the modifications of gear tooth profile.

Generally gears can be manufactured with different type of pressure angles, say, $14½^0$ $20^0$ and $25^0$ in industrial applications. In this research, the above three different pressure angles have been

ISSN: 2277-9655
Impact Factor: 1.852

selected for analysis. Influence of pressure angle in contact and root stresses has been analyzed earlier. This research is being carried out to understand the influence of pressure angle in vibration.

## 2 Vibration in Spur Gears

Vibrations in gears can be analyzed as repeatedly applied force acting on the gear tooth with respect to time, which tends to vibrate the gear. The force analysis on the gear is analyzed by considering the gear tooth as cantilever beam. The root of the tooth is considered as fixed end and at the other end, the loads are applied in vertical (transmitted load) and horizontal (radial load) direction as shown in figure – 08. The gear tooth displacement is defined by a term δ where W is the transmitted load applied on the tooth, L is the height of the tooth, E is the Modulus of Elasticity and I is the Area Moment of Inertia. The static deflection of the gear tooth is being considered for the natural frequency and it is found to be

$$\delta = \frac{WL^3}{3EI}$$

$$f_n = \frac{0.4985}{\sqrt{\delta}}$$

The natural frequency of the gear can be derived by considering the gear tooth model has a cantilever beam as shown in figure – 08 and according to Euler-Bernoulli hypothesis, the differential equation that satisfies the above loading condition is,

$$\frac{d^2}{dx^2}\left[EI(x)\frac{d^2y}{dx^2}\right] + E_f\, y - q(x) = 0 \qquad \text{..... (01)}$$

For $0 < \boldsymbol{x} < L$. the equation arises in the study of elastic bending of beams. Where ***y*** denotes the transverse deflection of the tooth, L is the length of the Gear tooth from the centre of the gear and ***EI*** denotes the flexural density, $\boldsymbol{E_f}$ is the foundation modulus and ***q(x)*** is the transverse load distributed along the tooth face and flank. The equation contains the fourth order derivative; it has to be integrated twice by parts to distribute the derivatives equally between the dependent variable *y* and the weight function ***v***. In this case ***v*** must be twice differentiable and satisfy the homogeneous form of an Essential Boundary condition. Multiplying the above equation by ***v*** and integrating the first term by parts twice with respect to ***x***, the following expression can be obtained,

$$\int_0^L\left(\frac{d^2v}{dx^2}EI\frac{d^2y}{dx^2} + E_f vy - vq\right)dx + \left[v\frac{d}{dx}\left(EI\frac{d^2y}{dx^2}\right) - \frac{dv}{dx}EI\frac{d^2y}{dx^2}\right]_0^L \qquad \text{...... (02)}$$

From the above equation, the specification *y* and $\left[\frac{dy}{dx}\right]$ constitutes the essential boundary conditions and

$\left[EI(x)\frac{d^2y}{dx^2}\right]$ is the bending moment, constitutes the natural boundary condition.

$$\int_{x_e}^{x_{e+1}}\left(EI\frac{d^2v}{dx^2}\frac{d^2y}{dx^2} + c_f vy - vq\right)dx - v(x_e)Q_1^e - \left(-\frac{dv}{dx}\right)\Big|_{x_e} Q_2^e - v(x_{e+1})Q_3^e - \left(-\frac{dv}{dx}\right)\Big|_{x_{e+1}} Q_4^e = 0 \qquad \text{........... (03)}$$

Now considering the Gear tooth, assuming the left extreme end of the gear tooth is fixed and the right end is free where it is subjected to transverse force and bending moment at x = L.
For the weak formulation, the functional, known as the total potential energy of the beam, is obtained using

$$I(w) = \int_0^L\left[\frac{b}{2}\left(\frac{d^2y}{dx^2}\right)^2 + \frac{E_f}{2}y^2 - qy\right]dx - y(L)F_o + \left(\frac{dy}{dx}\right)_{x=L} M_o \qquad \text{....... (04)}$$

In the euler Bernoulli beam theory, it is assumed that the plane cross sections perpendicular to the axis of the beam remains plane and perpendicular to the axis even after deformation. A small discretized element of the gear tooth can be isolated and the weak form of the solution can be arrived by modifying the above equations in to the following form,

$$\int_{x_e}^{x_{e+1}}\left(\frac{d^2v}{dx^2}EI\frac{d^2y}{dx^2}+E_f vy-vq\right)dx+\left[v\frac{d}{dx}\left(EI\frac{d^2y}{dx^2}\right)-\frac{dv}{dx}EI\frac{d^2y}{dx^2}\right]_{xe}^{x_{e+1}} \quad \ldots\ldots. (05)$$

Where *v(x)* is the weight function, which is twice differentiable with respect to *x*. The secondary variables

$$Q_1^e=\left[\frac{d}{dx}\left(EI\frac{d^2y}{dx^2}\right)\right]\Big\langle\ \Big|x_e=-V(x_e) \qquad Q_2^e=\left[\left(EI\frac{d^2y}{dx^2}\right)\right]\Big\langle\ \Big|x_e=-M(x_e) \qquad Q_{s3}^e=\left[-\frac{d}{dx}\left(EI\frac{d^2y}{dx^2}\right)\right]\Big\langle\ \Big|x_{e+1}=V(x_{e+1})$$

$$Q_4^e=-EI\left(\frac{d_2y}{dx^2}\right)\Big\langle\ \Big|x_{e+1}=M(x_{e+1}) \quad \ldots\ldots\ldots\ldots\ldots(06)$$

Which are consistent with the sign conventions for the above equations and the equation (05) can be rewritten as

$$\int_{x_e}^{x_{e+1}}\left(EI\frac{d^2v}{dx^2}\frac{d^2y}{dx^2}+c_f vy-vq\right)dx-v(x_e)Q_1^e-\left(-\frac{dv}{dx}\right)\Bigg|_{x_e}Q_2^e-v(x_{e+1})Q_3^e-\left(-\frac{dv}{dx}\right)\Bigg|_{x_{e+1}}Q_4^e=0 \quad \ldots.. (07)$$

In the above equation $Q_1^e$, $Q_3^e$ represents shear forces and $Q_2^e$, $Q_4^e$ represents the bending moments. The corresponding displacements and rotations are called generalized displacements.
Since there are four conditions in an element (two per node), a four parameter polynomial must be selected, there fore

$$y(x)=y_h^e(x)=a_1^e+a_2^e x+a_3^e x^2+a_4^e x^3 \quad \ldots.. (08)$$

From this equation, we derived the following hermite interpolation functions,

$$N_{c1}^e=1-3\left(\frac{x-x_e}{h_e}\right)^2+2\left(\frac{x-x_e}{h_e}\right)^3 \qquad N_{c2}^e=-(x-x_e)\left(1-\frac{x-x_e}{h_e}\right)^2 \qquad N_{c3}^e=3\left(\frac{x-x_e}{h_e}\right)^2-2\left(\frac{x-x_e}{h_e}\right)^3 \qquad N_{c4}^e=-(x-x_e)\left[\left(\frac{x-x_e}{h_e}\right)^2-\frac{x-x_e}{h_e}\right]$$

The finite element model of the Gear tooth can be obtained by substituting the above interpolation functions in the equation (06), for ***w*** and $N^e_j$ for the weight function *v* in to the weak form. The finite element model equation is

$$\sum_{j=1}\underbrace{\int_{x_e}^{x_{e+1}}\left(EI\frac{d^2\phi_i^e}{dx^2}\frac{d^2\phi_j^e}{dx^2}+c_f\phi_i^e\phi_j^e\right)dx}_{K_{ij}^e}\,u_j^e-\underbrace{\int\phi_i^e q\,dx-Q_i^e}_{F_i^e}=0$$

$$[K^e]=\frac{2E_eI_e}{l_e^3}\begin{bmatrix}6 & -3l_e & -6 & -3l_e\\ -3l_e & 2l_e^2 & 3l_e & l_e^2\\ -6 & 3l_e & 6 & 3l_e\\ -3l_e & l_e^2 & 3l_e & 2l_e^2\end{bmatrix}+\frac{E_f l_e}{420}\begin{bmatrix}156 & -22l_e & 54 & 13l_e\\ -22l_e & 4l_e^2 & -13l_e & -3l_e^2\\ 54 & -13l_e & 156 & 22l_e\\ 13l & -3l_e^2 & 22l_e & 4l_e^2\end{bmatrix} \quad \ldots\ldots\ldots(09)$$

By considering ***EI*** and ***q*** are constant over an element the element stiffness matrix [$\boldsymbol{K^e}$] and the force vector {$\boldsymbol{F^e}$} have the following specific forms for the element displacement and force degrees of freedom. Hence for finding out the natural frequency of the Gear tooth, $\boldsymbol{E_f}$ can be replaced with the term $\boldsymbol{-\omega^2\rho A}$.

$$[K^e]=\left\{\begin{matrix}\dfrac{2EI_e}{l_e^3}\begin{bmatrix}6 & -3l_e & -6 & -3l_e\\ -3l_e & 2l_e^2 & 3l_e & l_e^2\\ -6 & 3l_e & 6 & 3l_e\\ -3l_e & l_e^2 & 3l_e & 2l_e^2\end{bmatrix}-\omega^2\dfrac{\rho A l_e}{420}\begin{bmatrix}156 & -22l_e & 54 & 13l_e\\ -22l_e & 4l_e^2 & -13l_e & -3l_e^2\\ 54 & -13l_e & 156 & 22l_e\\ 13l & -3l_e^2 & 22l_e & 4l_e^2\end{bmatrix}\\ -\omega^2\dfrac{\rho I}{30l_e}\begin{bmatrix}36 & -3l_e & -36 & -3l_e\\ -3l_e & 4l_e^2 & 3l_e & -l_e^2\\ -36 & 3l_e & 36 & 3l_e\\ -3l_e & -l_e^2 & 3l_e & 4l_e^2\end{bmatrix}\end{matrix}\right\}\begin{Bmatrix}w_1\\ \phi_1\\ w_w\\ \phi_2\end{Bmatrix}=\begin{Bmatrix}Q_1\\ Q_2\\ Q_3\\ Q_4\end{Bmatrix} \quad \ldots\ldots(10)$$

## 3 Involute Profile

ISSN: 2277-9655
Impact Factor: 1.852

&ConjugateAction:

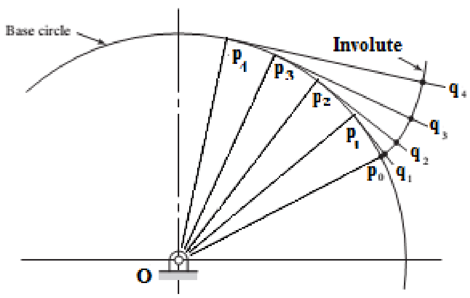


Figure – 01

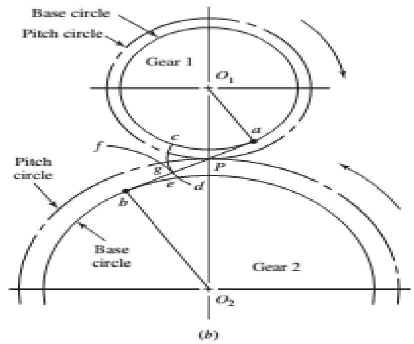


Figure – 02

To construct an involute curve as shown in Figure – 01, divide the base circle into a number of equal parts, and construct radial lines $op_0$, $op_1$, $op_2$, etc. Draw the lines $p_1q_1$, $p_2q_2$ perpendicular to $op_1$, $op_2$, respectively and it has to be continued for the rest of the lines. Lay off the distance $p_1p_0$ along the line $p_1q_1$. Similarly along the line $p_2q_2$, lay off double the line of $p_1p_0$. It has to be continued for the rest of the lines in the above same fashion. Through the points in the layoff, an involute curve can be constructed. When two gears are in mesh, it has purely rolling on the pitch circle but whereas it has sliding when it access or recess the path of contact. Considering the gear 1 as a pinion or driver gear rotates in counter clockwise and by constructing the pitch circles of radii $r_1$and $r_2$ as shown in figure – 02, which are tangent at the pitch point **P**, the line ***ab***, a common tangent, has been drawn through the pitch point. Line ***cd*** drawn through point P at an angle $\varphi$ to the common tangent ***ab*** is called the pressure line or the generating line or the line of action. It represents the direction in which the resultant force acts between the gears. The angle $\varphi$ is called the pressure angle.

## 4 Contact Ratio

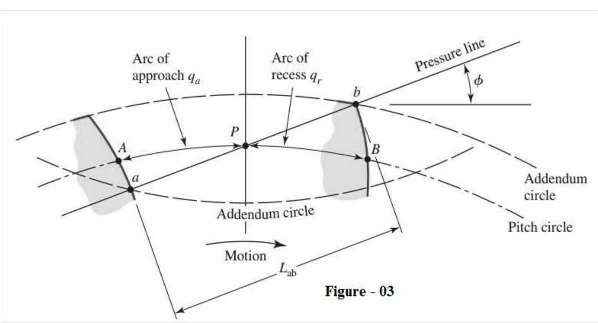


Figure - 03

A number which indicates the average number of pairs of teeth in contact is called contact ratio. This ratio is also equal to the length of the path of contact divided by the base pitch. Gears should generally be designed for a contact ratio of more than **1.2**, in order to reduce the vibration and noise as well as load jumping phenomenon on the successive tooth pairs.

$$\textbf{Contact Ratio} = \frac{L_{ab}}{p_c \cos\varphi}$$

Even inaccuracies in mounting might reduce the contact ratio, increasing the possibility of impact between the teeth. Contact ratio can be measured by considering the length of line of action $L_{ab}$ instead of the arc distance **AB**. The zone of action of meshing gear teeth is shown in figure – 03. Tooth contact begins and ends at the intersections of the two addendum circles with the pressure line. Initial contact occurs at ***a*** and final contact at ***b***. Tooth profiles drawn through these points intersects the pitch circle at **A** and **B**, respectively. The distance **AP** is called the arc of approach, and the distance **PB** is called the arc of recess. The sum of these is the arc of action $\mathbf{q_t}$. Now, consider a situation in which the arc of action is exactly equal to the circular pitch, that is, $\mathbf{q_t = p_c}$. This means that one tooth and its space will occupy the entire arc **AB**. In other words, when a tooth is just beginning contact at ***a***, the previous tooth is simultaneously ending its contact at **b**. Therefore, during the tooth action from **a** to **b**, there will be exactly one pair of teeth in contact. Next, consider a situation in which the arc of action is greater than the circular pitch, say, $\mathbf{q_t} = 1.2\ \mathbf{p_c}$. This means that when one pair of teeth is just entering contact at ***a***, another pair, already in contact, will not yet have reached ***b***. Thus, for a short period of time, there will be two teeth in contact, one in the vicinity of **A** and another near **B**. As the meshing proceeds, the pair near B must cease contact, leaving only a single pair of contacting teeth, until the procedure repeats itself.

## 5 Gear Modelling & Analysis

Pressure angle selection is based on the gear models which are in major applications.$14½^0$ (figure–09), $20^0$(figure – 10) and $25^0$ (figure – 11) are the three pressure angles which are selected for this analysis. For simplicity and ease of understanding, the $14½^0$, $20^0$ and $25^0$ pressure angled gears are mentioned here after as Gear H, Gear A and Gear T respectively for the analysis. The gear is selected based on the power and speed at the drive of application. An external spur gear made of EN24 steel is selected and it is modeled using modeling software with the specifications given in the table – 01. The gears are 36 teeth with the face width of 25.4mm and the pitch circle diameter of 114.3mm. Initially the gears are designed with the power of 3.75kW with a speed of 1500rpm. The torque for the selected power is calculated as 25Nm. The transmitted and radial load of the gear for the above input torque is 436N and 159N respectively. Gears are designed based on the Lewis and Buckingham equation models. The gears are checked and found satisfactory by comparing the wear load capacity and the beam strength of the gear with that of the buckingham's dynamic load. Though the gears are designed for the normal operating torque of the above, the gears are tested for ¼ , ½ , ¾ , full load, 1½ times and double the operating torque, i.e. 6.25Nm, 12.5Nm, 18.75Nm, 25Nm, 37.5Nm and 50Nm. For all the above toques, the concerned transmitted and radial loads are calculated and it is given in the gear tooth. The 3D model generated gear is discretized into 20 noded tetra-hedral elements. And the modal frequencies are calculated first for all the gears. The fundamental natural frequencies of the gears H, A and T are 7706Hz, 7694Hz and 7107Hz respectively. Since all the gears are having a high natural frequency when comparing with the forcing frequency of 900Hz (Gear Meshing Frequency), the gear system may not fail due to resonance. But of course, it happens if the gear shaft operates at resonance. The gears are analyzed under Frequency Response Analysis in the range of 0 to 3600Hz for an interval of 20 modes. The range has been selected based on the gear mesh frequency as given in table – 02. The vibration limit for the above selected spur gear is 12.5mm/sec as per the ANSI/AGMA 6000 – B96 Standards [ ] for the above mentioned meshing frequency. An experimental analysis has also been done to compare and check the computed value and the results are in good agreement. The discretization has been done by using FEA Coding software. A cylindrical support for the gear is given at the centre of the gear i.e. at the hole provided for the shaft in the analysis. The forces are given in the tooth as shown in figure – 08. The results obtained from the model are created in a tabular form and a graph has been generated in excel format to understand the vibration damping capacity of these gears.

ISSN: 2277-9655
Impact Factor: 1.852

# 6 Results and Discussion

## *6.1 ANALYSIS ALONG THE RADIAL LOAD DIRECTION:*

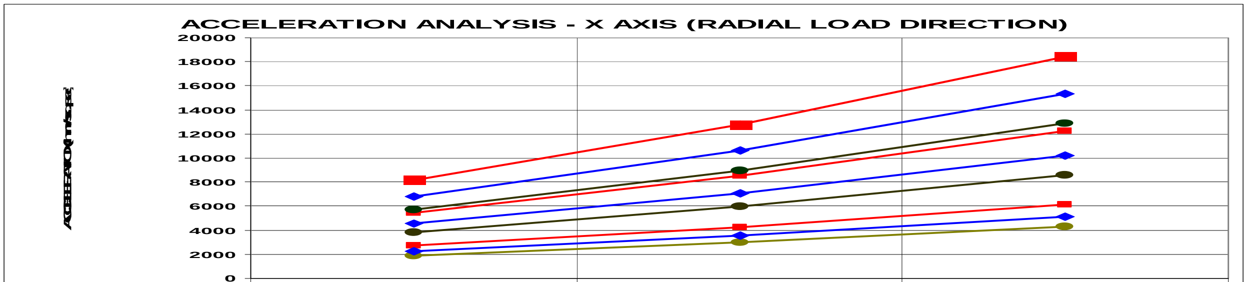


| | 720 | 900 | 1080 |
|---|---|---|---|
| 6.25Nm 14.5DEG | 2724 | 4258.3 | 6135.6 |
| 6.25Nm 20DEG | 1905.7 | 2978.9 | 4291.9 |
| 6.25Nm 25DEG | 2267.4 | 3545.6 | 5110.8 |
| 12.5Nm 14.5DEG | 5448 | 8516.6 | 12271 |
| 12.5Nm 20DEG | 3811.4 | 5957.9 | 8583.8 |
| 12.5Nm 25DEG | 4534.8 | 7091.3 | 10222 |
| 18.75Nm 14.5DEG | 8172 | 12775 | 18407 |
| 18.75Nm 20DEG | 5717.2 | 8936.8 | 12876 |
| 18.75Nm 25DEG | 6802.2 | 10637 | 15332 |

Figure – 04

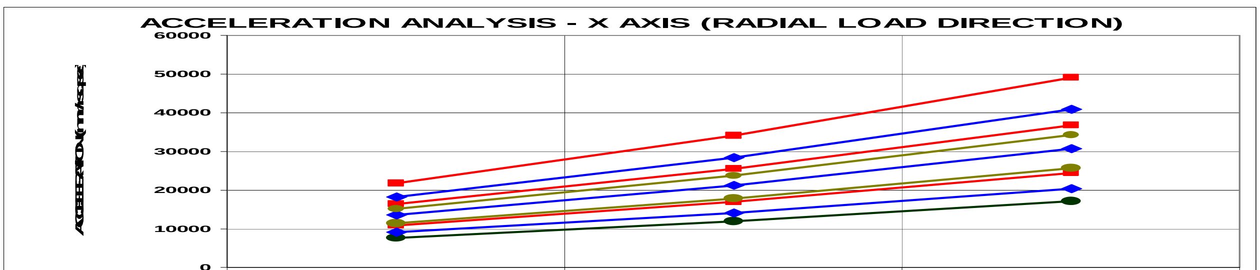


| | 720 | 900 | 1080 |
|---|---|---|---|
| 25Nm 14.5DEG | 10896 | 17033 | 24542 |
| 25Nm 20DEG | 7622.9 | 11916 | 17168 |
| 25Nm 25DEG | 9069.6 | 14183 | 20443 |
| 38Nm 14.5DEG | 16347 | 25554 | 36819 |
| 38Nm 20DEG | 11434 | 17874 | 25751 |
| 38Nm 25DEG | 13604 | 21274 | 30665 |
| 50Nm 14.5DEG | 21792 | 34067 | 49085 |
| 50Nm 20DEG | 15246 | 23831 | 34335 |
| 50Nm 25DEG | 18139 | 28365 | 40886 |

Figure – 05

The radial load is applied along the X axis direction (figure – 08). Figure - 04 represents the acceleration analysis in the radial load direction i.e. X axis direction for these three types of spur gears, when the load applied is from 6.25Nm to 18.75Nm. In this analysis, gear H is attaining the maximum value of 8.357m/s$^2$ at the frequency of 1260Hz. But for the operating frequency of 720, 900 and 1080Hz, it reaches to a maximum of 2.724, 4.258 and 6.135m/s$^2$ at the load of 6.25Nm. Whereas at the same load and at the same frequencies, gear T reaches to a maximum value of acceleration of 2.267, 3.545 and 5.110m/s$^2$. Almost 20% of the amplitude of acceleration is getting reduced due to the pressure angle increase. But at the same time, better than this gear T, the normal gear which is used commercially having 20$^0$ pressure angle i.e. gear A is more conveniently operating at an acceleration of 1.9, 2.9 and 4.3m/s$^2$ which is considerable reduced the amplitude of vibration. The gear A reduces the amplitude almost 45% from the gear H. Now this amplitude of vibration reduction is exists in all the load conditions from 6.25Nm to 18.75Nm. For these cases, the highest amplitudes are always in the gear H which is unexpectedly increases more, i.e. the variation in the amplitude between the

ISSN: 2277-9655

Impact Factor: 1.852

remaining two gears with the gear H is non-linearly varying from the first load set up to the final load setup. At the load of 18.75Nm, the gear H is accelerated to 8.1, 12.7 and18.4 $m/s^2$ for the operating frequencies of 720,900 and 1080Hz. For the same load and speeds, the gear A reaches only 5.7, 8.9 and 12.8$m/s^2$. It shows that the gear A reaches the same value of gear H but at the frequency higher than the gear H, i.e. at the frequency of 900Hz gear H touches 12.7$m/s^2$ , but the same amplitude is attained by the gear A only at the frequency of 1080Hz.

The analysis has continued upto 50Nm as shown in figure – 05. At the regular operating torque of 25Nm, the gear F attains 10.9$m/s^2$ at 1200rpm(720Hz) and 17$m/s^2$ at an operating speed of 1500rpm (normal running speed-900Hz), it shows that the acceleration level is crossing 9.81$m/s^2$(1g), which produces slighting aggressive fluctuation in the gear shaft. Also, when it reaches 1080Hz i.e. 1800rpm, the Gear H reaches to a maximum of 24.5$m/s^2$. Whereas for the same load, the gear T attains only 9,14 and 20 $m/s^2$ for the frequency of 900 and 1080Hz. Even gear T has also having more amplitude of acceleration but having a better control than Gear H. but gear A has very good control and it attains only 7.6, 11.9 and 17.1$m/s^2$ at the operating frequency of 720Hz,900Hz and 1080Hz respectively. At the highest load i.e. at double the operating torque (50Nm), the gear H attains 49$m/s^2$ at 1080Hz and 34$m/s^2$ at 900Hz. In this load, the gear A attains only 34.3$m/s^2$ at 1080Hz and 23.8$m/s^2$ at 900Hz which is considerably lesser than the gear H and also even at 1.5times of the normal torque i.e. 38Nm, the gear H attains the magnitude of acceleration which is higher than the gear A's amplitude even at 50Nm. Gear A attains only 23.8$m/s^2$ at 900Hz at 50Nm, but gear H attains 34$m/s^2$ at 50Nm at 25.6$m/s^2$ at 38Nm, for the same operating frequency. From the data given in figure – 05, it is concluded that, for a better vibration control, Gear A having $20^0$ pressure angle is most worthwhile and Gear F can also be considered better than gear H. Even the smallest error in the pressure angle can create a large amount of variation in the magnitude of vibration of the gear system.

*6.2 ANALYSIS ALONG THE TRANSMITTED LOAD DIRECTION:*

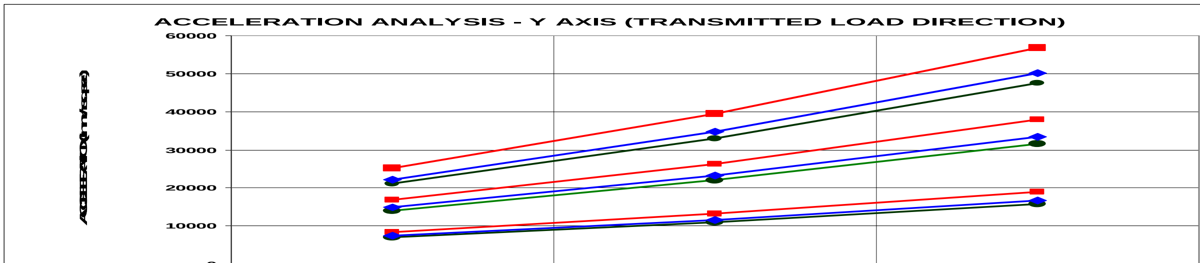


| | 720 | 900 | 1080 |
|---|---|---|---|
| 6.25Nm 14.5DEG | 8406.3 | 13146 | 18951 |
| 6.25Nm 20DEG | 7017.7 | 10976 | 15825 |
| 6.25Nm 25DEG | 7414.5 | 11600 | 16729 |
| 12.5Nm 14.5DEG | 16813 | 26292 | 37901 |
| 12.5Nm 20DEG | 14035 | 21952 | 31650 |
| 12.5Nm 25DEG | 14829 | 23199 | 33458 |
| 18.75Nm 14.5DEG | 25219 | 39438 | 56852 |
| 18.75Nm 20DEG | 21053 | 32928 | 47474 |
| 18.75Nm 25DEG | 22244 | 34799 | 50187 |

FREQUENCY(Hz)

Figure – 06

ISSN: 2277-9655

Impact Factor: 1.852

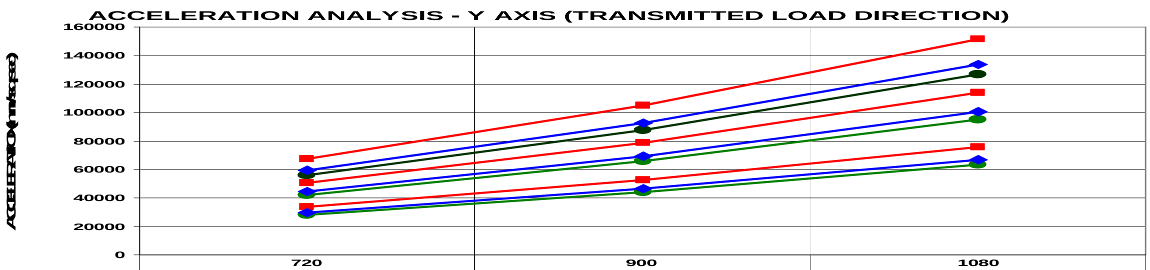


| | 720 | 900 | 1080 |
|---|---|---|---|
| 25Nm 14.5DEG | 33625 | 52585 | 75802 |
| 25Nm 20DEG | 28071 | 43904 | 63299 |
| 25Nm 25DEG | 29658 | 46398 | 66915 |
| 38Nm 14.5DEG | 50430 | 78865 | 1.14E+05 |
| 38Nm 20DEG | 42106 | 65856 | 94949 |
| 38Nm 25DEG | 44487 | 69597 | 1.00E+05 |
| 50Nm 14.5DEG | 67250 | 1.05E+05 | 1.52E+05 |
| 50Nm 20DEG | 56142 | 87808 | 1.27E+05 |
| 50Nm 25DEG | 59316 | 92796 | 1.34E+05 |

FREQUENCY(Hz)

Figure – 07

The Transmitted load is applied along the Y axis direction (figure – 08). Figure – 06 represents the acceleration analysis in the Transmitted load direction i.e. Y axis direction for these three types of spur gears, when the load applied is from 6.25Nm to 18.75Nm. In this analysis, gear H is attaining the maximum value of 56.85m/s$^2$ at the frequency of 1080Hz at a load of 18.75Nm. But for the operating frequency of 720, 900 and 1080Hz, it reaches to a maximum of 8.4m/s$^2$, 13m/s$^2$ and 19m/s$^2$ at the load of 6.25Nm. Whereas at the same load and at the same frequencies, gear T reaches to a maximum value of acceleration of 7.4, 11.6 and 16.7m/s$^2$. Almost 13% of the amplitude of acceleration is getting reduced due to the pressure angle increase. The normal gear which is used commercially having 20$^0$ pressure angle i.e. gear A is also operating almost with the same value of acceleration. At the load of 18.75Nm and the frequencies of 720, 900 and 1080Hz, the gear H attains 25, 40 and 57m/s$^2$. The gear T attains 22, 35 and 50m/s$^2$. And the gear A attains only 21, 33 and 47m/s$^2$. It shows that the gear T has reduced the amplitude almost 12%. And the gear A is reducing the amplitude of vibration around 20%, when comparing with gear H. At the operating torque of 25Nm, the gear H reaches to a value of 34, 53 and 76m/s$^2$. The gear T touches the value of 30, 46 and 67m/s$^2$. Whereas the normal 20$^0$ pressure angled gear A attains to a maximum of 28, 43 and 63m/s$^2$. In this analysis, the gear T reduces the amplitude to 12% and gear A reduces to 18%.

The analysis has continued upto 50Nm as shown in figure – 07. At double the operating torque i.e. 50Nm, the gear H attains 67m/s$^2$ at 1200rpm(720Hz) and 105m/s$^2$ at an operating speed of 1500rpm (normal running speed-900Hz), which produces more aggressive fluctuation in the gear shaft. Also, when it reaches 1080Hz i.e. 1800rpm, the Gear H reaches to a maximum of 152m/s$^2$. Whereas for the same torque, the gear T attains only 93 and 134m/s$^2$ for the frequency of 900 and 1080Hz. Even gear T has also having higher amplitude of acceleration, but having a better control than Gear H. but gear A has very good control and it attains only 56, 88 and 127m/s$^2$ at the operating frequency of 720Hz,900Hz and 1080Hz respectively. The reduction of amplitude is almost 17% comparing to the gear H. From the data given in figure – 06 and 07 , it is concluded that, for a better vibration control, Gear A having 20$^0$ pressure angle is most worthwhile and Gear F can also be considered better than gear H.

ISSN: 2277-9655
Impact Factor: 1.852

# 7 Conclusion

The above variations in the amplitude of vibration in both Transmitted load and radial load direction indicates that even the very small modifications in pressure angle for betterment of the gear vibration damping influences much. Even the manufacturing errors can also leads to a certain amount of contribution to the amplitude of vibration. Hence it is concluded from the above discussions that the pressure angle influence must be accountable for the vibration measurement in a considerable parameter.

# 8 Figures

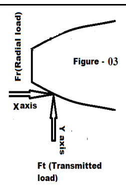


Figure– 08

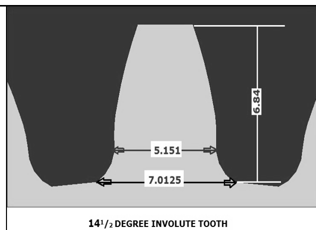


Figure – 09

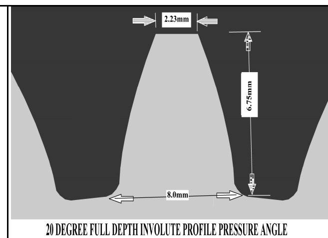


Figure – 10

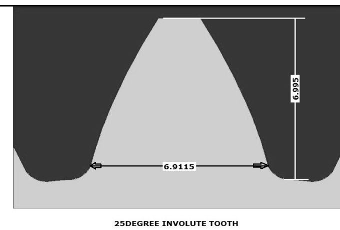


Figure – 11

Figure 1, Definition of floor plan and usage - using the style "*Caption*"

# 9 Tables

| **Table – 01 Range of Frequency to be measured for Spur Gear Vibration** | | | | | | |
|---|---|---|---|---|---|---|
| Gear Mesh Frequency (GMF) = 900Hz(Speed X No. of Teeth)<br>Maximum Frequency (Fmax.)=2475Hz.(2.75 X GMF) All the below mentioned values are in Hz. | | | | | | |
| Band Low Frequency | 1% of Fmax. | 0.1GMF | 0.25GMF | 0.75GMF | 1.25GMF | 1.75GMF |
| | 24.75Hz | 90Hz | 225Hz | 675Hz | 1125Hz | 1575Hz |
| Band High Frequency | 0.1GMF | 0.25GMF | 0.75GMF | 1.25GMF | 1.75GMF | 100%Fmax. |
| | 90Hz | 225Hz | 675Hz | 1125Hz | 1575Hz | 2475Hz |
| % of Overall Band Alarm | 90% | 40% | 30% | 70% | 30% | 50% |
| Description | Lower Harmonics | Higher Harmonics | 0.5 GMF &Sidebands | GMF & sidebands | 1.5GMF &Sidebands | 2 & 2.5GMF &Sidebands |

**TABLE – 02**

**GEAR PARAMETERS**

| | | | |
|---|---|---|---|
| Module(***m***) | 3.175mm | Pitch Circle Diameter(m) | 0.114 |
| Spur Gear type | $20^0$ full depth | No. of Teeth | 36 |
| Addendum | 1***m*** (3.175mm) | Gear Material | EN24 steel |
| Deddendum | 1.25 ***m***(3.969mm) | Quality of a gear | ISO Quality 8 |
| Clearance | 0.25 ***m***(0.794mm) | Power (kW) | 3.75 |
| Working depth | 2***m***(6.35mm) | Gear Ratio | 1:1 |
| Whole depth | 2.25***m***(7.1438mm) | Young's Modulus ($N/m^2$) | 2 e+011 |
| Tooth thickness | 1.571***m***(4.988mm) | Density ($kg/m^3$) | 7850 |
| Face width | 8***m***(25.4mm) | Poisson's Ratio | 0.3 |
| Fillet radius (minimum) | 0.3 ***m***(0.953mm) | Tensile Strength($N/m^2$) | $460 \times 10^6$ |
| Top land (minimum) | 0.25***m***(0.794mm) | Compressive strength($N/m^2$) | $250 \times 10^6$ |

# Acknowledgements

Corresponding Author thanks MAGTORQ (P) Ltd., Hosur, India for giving the support to make the research in gear vibrations.

# References

Woohyung Kima, Hong Hee Yoo, Jintai Chung, Dynamic analysis for a pair of spur gears with translational motion due to bearing deformation, *Journal of Sound and Vibration* 329 (2010) 4409–4421.

M. Amabili, A. Fregolent, A method to identify modal parameters and gear errors by vibrations of a spur gear pair, *Journal of Sound and Vibration*, 214(2) (1998) 339–357.

P. Velex, M. Maatar, A mathematical model for analyzing the influence of shape deviations and mounting errors on gear dynamic behavior, *Journal of Sound and Vibration*, 191 (5) (1996) 629–660.

Gang Liu and Robert G. Parker, Dynamic Modeling and Analysis of Tooth Profile Modification for Multi-mesh Gear Vibration, *Journal of Mechanical Design* – ASME, (2008) Vol. 130/ 121402-1.

Giorgio Bonori, Marco Barbieri and Francesco Pellicano, Optimum profile modifications of spur gears by means of genetic algorithms, *Journal of Sound and Vibration,*

Giorgio Bonori, Francesco Pellicano, Non-smooth dynamics of spur gears with manufacturing errors, *Journal of Sound and Vibration, 306 (2007) 271–283.*

A. Kahraman, R. Singh, Nonlinear dynamics of a spur gear pair, *Journal of Sound and Vibration* 142 (1) (1990) 49–75.

Jaakko Kleemola, Arto Lehtovaara, Experimental simulation of gear contact along the line of action, *Tribology International*, 42 (2009) 1453–1459.

A. Bracci, M. Gabiccini, A. Artoni, M. Guiggiani, Geometric contact pattern estimation for gear drives, Comput. Methods Appl. Mech. Engrg. 198 (2009) 1563–1571.

Fatih Karpat, Stephen Ekwaro-Osire, Kadir Cavdar, Fatih C. Babalik, Dynamic analysis of involute spur gears with asymmetric teeth, *International Journal of Mechanical Sciences*, 50 (2008) 1598–1610.

Olek C Zienkiewicz, Robert L Taylor,The Finite Element Method for Solid and Structural Mechanics, Sixth Edition.